Observation of Disorder-Induced 2D Mott-Hubbard States of the Alkali-Earth Metal (Mg,Ba)-Adsorbed Si(111) Surface

J. R. Ahn, S. S. Lee, N. D. Kim, J. H. Min, C. G. Hwang, and J. W. Chung
Physics Department and Basic Science Research Institute, Pohang University of Science and Technology, San 31 Hyoja Dong, Pohang 790-784, Korea
(Received 14 June 1999)

We report evidence of a disorder-driven Mott-Hubbard-type localization on the alkali-earth metal (AEM) (Mg,Ba)-adsorbed Si(111)-(7 × 7) surface. The clean metallic Si(111) surface is found to undergo a two-dimensional (2D) metal-insulator transition as randomly distributed AEM adsorbates cause disorder on the surface. A well-defined electron-energy-loss peak unique to the insulating phase is attributed to an interband excitation between the split Hubbard bands originated from a metallic surface band at Fermi energy. A quantitative analysis of the loss peak reveals that the AEM-induced insulating surfaces are of a Mott-Hubbard type driven essentially by disorder.

PACS numbers: 71.30.+h, 71.20.Dg, 73.20.–r

Anderson [1] predicted that the presence of disorder in a noninteracting electron system may drive a metallic state into an insulating state (gapless Anderson insulator) by localizing all the states at Fermi energy E_F. Since this early prediction, a number of researchers have extended this notion to various correlated electron systems [2–6]. For an interacting electron system in the absence of perturbations such as disorder and lattice distortions, a metal-insulator transition (MIT) can occur by a delicate interplay between the intrasite Coulomb repulsion U and the nearest neighbor intersite hopping energy t. When $U \gg t$, a metal can be a Mott-Hubbard insulator or a polaron-type insulator depending on the absence or the presence of a local lattice distortion, respectively. Several such examples have been reported to date for two-dimensional (2D) correlated electron systems [7–16]. When disorder is introduced to a 2D correlated system in the form of random site potential W, a 2D MIT becomes more intriguing. Yi *et al.*, based on a 2D Anderson-Hubbard model, predicted that a 2D metallic state may transform into either a Mott-Hubbard or a gapless Anderson insulating state depending on the relative strength of U/W with respect to t/W [3]. No experimental realization of a 2D system, however, exhibiting an insulating state of correlated electrons caused by disorder has been reported yet to our knowledge despite the theoretical expectation [2–6].

Here we report such a case where disorder drives a 2D metallic surface into a 2D Mott-Hubbard-type insulator [17]. The 2D systems are alkali-earth metal (AEM) adsorbed Si(111) surfaces, which have been investigated primarily by using high-resolution electron-energy-loss spectroscopy (HREELS). A Si(111)-(7 × 7) (hereafter Si-7 for brevity) surface was chosen because of its ordered 2D metallic nature composed of a crystalline array of half-filled dangling bonds acting as one-electron centers. Moreover, the bandwidth ($w \sim 0.2$ eV) of its metallic surface band [18] is almost comparable to U so that the surface becomes susceptible to an external perturbation to trigger such an MIT.

HREELS measurements were carried out in an ultrahigh vacuum (UHV) chamber of base pressure below 3×10^{-11} mbar utilizing a Leybold-Heraeus ELS-22 spectrometer of an optimum resolution of 8 meV and a half-acceptance angle of 2°. The degree of disorder caused by AEM adsorbates was examined by measuring the change of a seventh-order low-energy-electron diffraction (LEED) spot of the clean metallic Si-7 surface. The LEED optics used is a high-spatial-resolution LEED (Leybold SPA-LEED) system which has a nominal transfer width of ~1200 Å. The AEM-induced changes in the valence band of the Si-7 surface were measured by photoelectron spectroscopy using synchrotron photons of energy 20 eV at the beam line 2B1, Pohang Light Source. Mg was thermally evaporated from a Mg rod while a commercial SAES dispenser was used as a Ba source. The AEM sources were thoroughly outgassed to maintain the chamber pressure below 1×10^{-10} mbar during AEM evaporation. The adsorbate coverage θ was estimated by measuring the change in work function $\Delta\phi$ as a function of AEM exposure. The saturation coverage where the metallic excitation continuum reappears in EELS spectra was estimated as 1 monolayer (ML). Experimental details will appear elsewhere in a longer paper.

Progressive evolution of the (1/7,0) LEED spot with increasing AEM coverage θ at room temperature is presented in Fig. 1(a) for Ba adsorption. One immediately notices that the spot weakens gradually with θ up to 0.5 ML. The intensity profiles in Fig. 1(a) are best described by a Lorentzian to the power 3/2, i.e., $I(k) = I_p/[(\frac{q-q_0}{\xi})^2 + 1]^{3/2}$, where I_p, q_0, and ξ are the peak intensity, the peak position, and the Lorentzian width of the (1/7,0) LEED spot [19]. The results of the fits shown in Fig. 1(b) indicate that the AEM adsorbates cause disorder on the surface as do random fields similarly in an Ising system [20,21].

 0031-9007/00/84(8)/1748(4)$15.00 © 2000 The American Physical Society

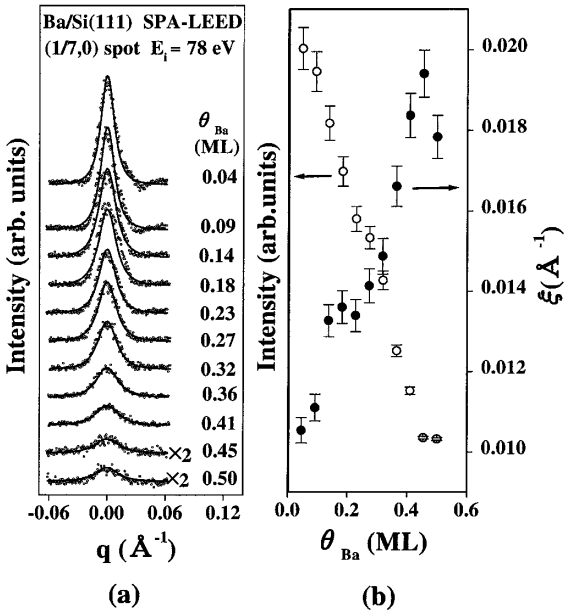

FIG. 1. (a) Progressive change of the (1/7,0) LEED spot with increasing Ba coverage. The solid curves are fitted curves. (b) Changes in the peak intensity (empty circles) and the full width at half maximum ξ (filled circles) with Ba coverage.

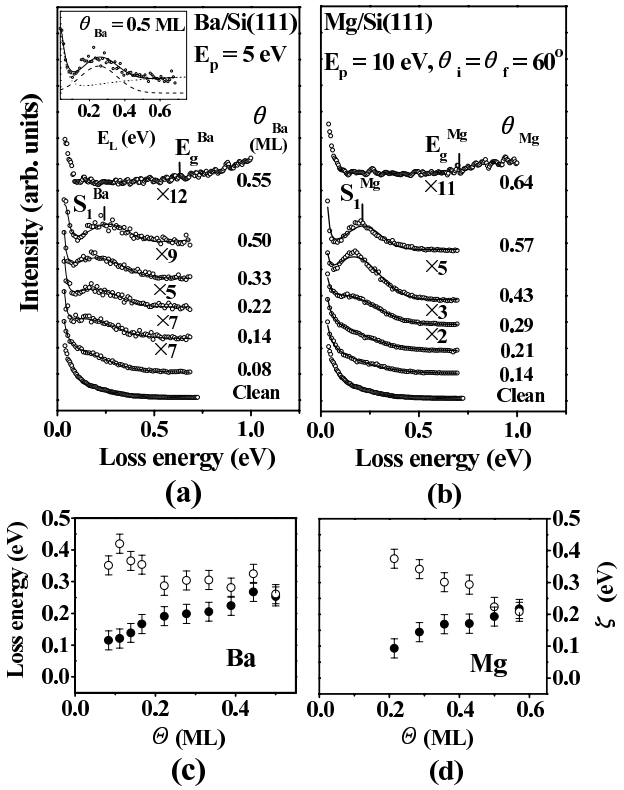

FIG. 2. Development of EELS features with (a) Ba and (b) Mg adsorption on the Si-7 surface. Evolution of the loss energy (filled circles) and the linewidth ζ (empty circles) of S_1 are shown in (c) for Ba and in (d) for Mg.

As disorder (or equivalently θ) increases on the surface, concomitant changes in electrical properties appear in the EELS spectra presented in Figs. 2(a) and 2(b) for the Ba- and Mg-adsorbed surfaces at room temperature, respectively. The extended tail of the elastic peak in the bottom spectra reveals the metallic nature of the clean Si-7 surface. Notice that a distinctive loss peak (S_1^{Ba} or S_1^{Mg} abbreviated as S_1 hereafter) appears at low AEM coverages. With increasing θ, S_1 shifts towards the higher loss energy side and disappears almost completely at the critical coverage $\theta_c = 0.55$ and 0.64 ML, where energy gaps of 0.62 eV (E_g^{Ba}) and 0.65 eV (E_g^{Mg}) are evident for Ba- and Mg-adsorbed surfaces, respectively. *The presence of such a nonvanishing energy gap indicates a 2D MIT caused by the AEM adsorption*. Although similar MIT's have been observed also for metal-adsorbed Si-7 surfaces [11–13], no clear explanation of the phenomena has been provided yet. In contrast, the insulating metal-adsorbed GaAs(110) surfaces have been well characterized, i.e., Na/GaAs(110) as a bipolaron-type insulator [15] and (Cs,K)/GaAs(110) as Mott-Hubbard-type insulators [8,16].

In order to understand the origin of the AEM-induced insulating states, we first attempt to analyze the loss peak S_1 by adopting the fitting procedure of a loss peak as discussed by Laitenberger and Palmer [22]. As an illustration of the fitting procedure, a Gaussian-fitted S_1 peak (dashed curve) after a polynomial background (dotted curve) subtraction is shown in the inset of Fig. 2(a). The results of the fits showing the evolution of the loss energy and the width of S_1 with θ are presented in Fig. 2(c) for Ba and in 2(d) for Mg. One finds that the loss energies gradually shift towards the higher energy side up to 0.25 and 0.22 eV with increasing θ while the linewidths decrease down to 0.26 and 0.21 eV for Ba- and Mg-adsorbed surfaces, respectively.

Having characterized the behavior of $S_1(\theta)$, we now discuss the origin of the S_1 loss peak. There are several possible sources for S_1 including a local AEM-Si vibrational excitation, a surface plasmon, a surface phonon, or an interband electronic excitation. All these sources except the interband excitation, however, are not quite likely as discussed briefly below. The significantly higher loss energies ($E_L \leq 260$ meV) and an order of magnitude broader linewidth of S_1 compared to the corresponding values of a typical metal-Si vibrational mode ($E_L \leq 25$ meV) [23,24] easily rule out the vibrational origin. Also it is not hard to show that several order of higher carrier concentrations are necessary to excite a surface plasmon of a similar energy in S_1. Finally the absence of multiphonon peaks in our spectra simply excludes the possibility of a single-phonon loss peak for S_1.

We now consider whether S_1 stems from an interband transition. Among the three surface bands characterizing a clean Si-7 surface [see Fig. 3(a) and Ref. [12]], the flat surface band S_m at E_F [25] from the half-filled Si adatoms is the only state that can be associated with S_1 since all

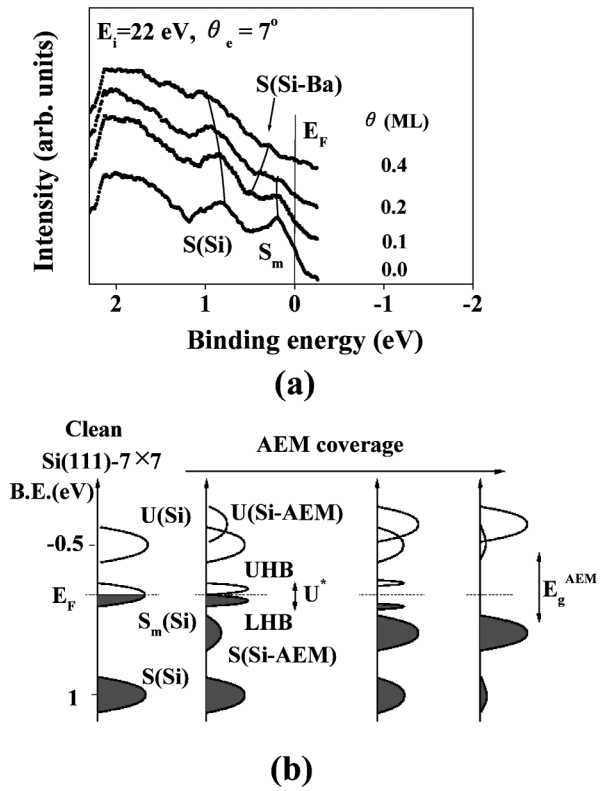

FIG. 3. (a) Progressive changes in the valence band of the Si-7 surface caused by Ba adsorption. (b) Schematic illustration of the splitting of the S_m band into upper and lower Hubbard bands (UHB and LHB) by the AEM adsorption.

other surface bands farther below E_F are located at energies already greater than the energy of S_1 [12]. This turned out to be true even after the adsorption of AEM atoms as seen in Fig. 3(a), where no surface band other than S_m itself apparently appears near E_F within the energy resolution ($\sim$140 meV). We thus are led to conclude that the splitting of the S_m band as illustrated schematically in Fig. 3(b) can explain the presence of S_1. Therefore S_1 is attributed to the interband transition between the split bands [LHB and UHB in Fig. 3(b)] of S_m. Interestingly a similar splitting of S_m due to the electron-electron correlation interaction has been ascribed to the temperature-induced MIT of the clean Si-7 surface [7]. Meanwhile the interband transition depicted in Fig. 3(b) between the Si-AEM hybridization bands is, in fact, observed as a broad loss peak at 1.2 eV (not presented in Fig. 2).

What then drives the splitting of S_m? Recent theoretical works [3–5] based on a 2D Anderson-Hubbard model show that not only the electron correlation interaction but also disorder in the form of random site potentials also causes an MIT. This occurs by localizing conduction electrons of a disordered 2D interacting electron system. The role of disorder in driving the localization in such a system is to modify both the intersite hopping energy t and the intrasite Coulomb repulsion U in such a way that U/t exceeds a certain critical value [3–5]. More specifically, a theoretical U/W versus t/W phase diagram obtained by Yi *et al.* using a quantum real space renormalization group method predicts a fixed point at $U/W = 7.3$ that separates a Mott-Hubbard regime ($U/W \rightarrow \infty$) from a gapless Anderson insulator regime [3]. Since the AEM-induced MIT occurs in parallel with the growing disorder, the AEM-induced disorder rather than the Si-AEM bonding itself is thought to drive the splitting of the S_m band into lower- and upper-Hubbard bands [Fig. 3(b)]. A good justification of the role of disorder (or W) is found by estimating the effective interaction parameters U_*/W and t_*/W modified by disorder since W is not a directly measurable quantity. To this end, we have utilized a relation derived by Zimanyi and Abrahams that couples t_* with W [see Eq. (1) below] [4].

Although the nonvanishing loss energy of S_1 itself suggests a Mott-Hubbard type rather than a gapless Anderson type for the AEM-induced insulating phases, we explore the insulating nature more quantitatively by determining an experimental U_*/W versus t_*/W phase diagram to compare with a theoretical one [3]. While $U_*(\theta)$ becomes known directly from the loss energy of S_1, $t_*(\theta)$ can be determined from the linewidth $\zeta(\theta)$ [see Figs. 2(c) and 2(d)] of S_1, which is a convolution product of the two bandwidths w_l and w_u of the split Hubbard bands. When $w_l(\theta) = w_u(\theta) = w(\theta)$ with a Gaussian line shape for w, $t_*(\theta)$ becomes $w(\theta)/2z = \zeta(\theta)/2\sqrt{2}\,z$ (z is a coordination number, 6 for a Si adatom) [2]. We now postulate $W(n_d) = c_1 n_d$, which is reasonable since the degree of disorder [represented by ξ in Fig. 1(b)] is almost linearly proportional to θ. Here $n_d \equiv \theta/\theta_c$ is a normalized AEM coverage and c_1 is a constant independent of n_d. Note that n_d denotes the fraction of saturated Si dangling bonds. For a triangular lattice consisting of the half-filled dangling bonds of the Si-7 surface, $t(n_d)$ behaves as $t(n_d) = t(0)\ \exp[c_2 r_0(1 - 1/\sqrt{1 - n_d})]$, where r_0 is the nearest neighbor distance of the unsaturated dangling bonds and c_2 is a constant [2]. We then estimate $W(n_d)$ by least-squares fitting $\zeta(n_d)$ [Fig. 4(a)] using

$$\zeta(n_d) = 12\sqrt{2}\,t(1 - W^2/4t^2)/(1 + W^2/t^2) + \zeta_0\,, \quad (1)$$

and taking c_1 and c_2 as fitting parameters [4]. Here $\zeta_0 = 0.035$ eV is the instrumental resolution of our HREELS system. Since $\zeta(n_d) \geq 10\ \zeta_0$ for most n_d in Fig. 4(a), the contribution of ζ_0 to $\zeta(n_d)$ is almost negligible ($\leq$0.5%).

The resulting values of U_*, t_*, and W obtained from the fittings [Fig. 4(a)] reveal the behavior of $U_*^2/16t_*^2$ versus n_d [Fig. 4(b)] and U_*/W versus t_*/W [Fig. 4(c)]. As expected, one finds the unique feature of a Mott-Hubbard insulator from the values of $U_*^2/16t_*^2$ satisfying a Harrison criterion $U_*^2 \geq 16t_*^2$ for all n_d. This indicates that U_* becomes enhanced whereas t_* is reduced with increasing n_d (or disorder). The experimental $U_*/W - t_*/W$ phase diagram in Fig. 4(c) provides a further insight to the nature

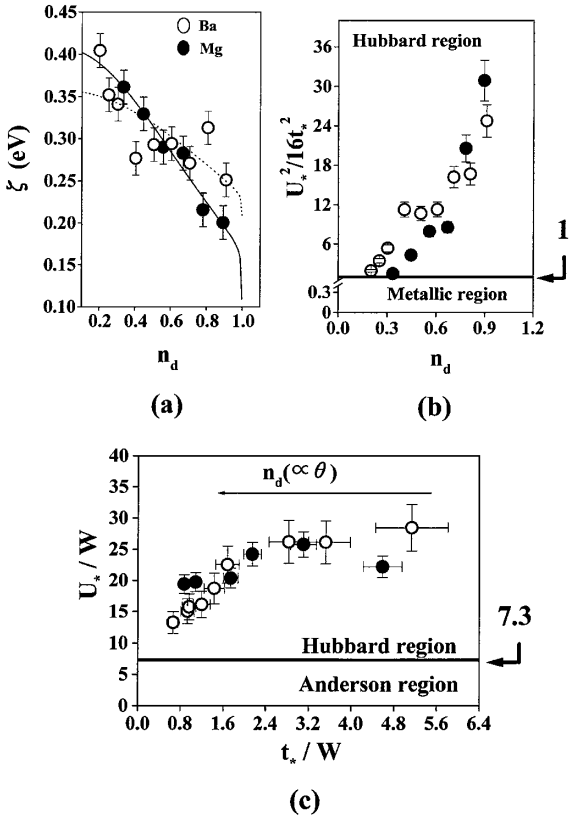

FIG. 4. (a) Changes of the linewidth (ζ) of S_1 with increasing n_d (the number of saturated Si dangling bonds). The solid (dotted) curve is a least-squares fit of the data for Mg (Ba) to estimate W from Eq. (1). (b) A plot of $U_*^2/16t_*^2$ vs n_d determined from EELS data. The presence of all the data in the Hubbard region ($U_*^2/16t_*^2 \geq 1.0$) reveals the insulating feature of the AEM-adsorbed Si-7 surfaces. (c) An experimental U_*/W vs t_*/W phase diagram. Again, all the data existing above the fixed point $U_*/W = 7.3$ demonstrate the nature of the Mott-Hubbard insulators.

of the localization: First, the nature of the Mott-Hubbard states is confirmed again by all the data existing above a fixed point of $U_*/W = 7.3$. Second, t_* is reduced much more rapidly than the enhanced U_* by disorder as suggested from the data points approaching the fixed point as n_d increases. This observation, in turn, implies a significantly reducing coupling constant ($J_* = 4t_*^2/U_*$) by increasing disorder [4], which might result in the localization of correlated electrons. We thus believe that *the AEM (Ba,Mg)-induced Mott-Hubbard insulating states of the Si-7 surface are a manifestation of the 2D disorder-induced localization of correlated electrons.*

In summary, we report a case where disorder produced by random adsorption of AEM adsorbates on a metallic Si-7 surface drives a 2D metal-insulator transition. Our results compared with recent theory indicate that the AEM-adsorbed Si-7 surfaces become Mott-Hubbard-type insulators primarily by the much more reduced t_* compared to the U_* enhanced by the AEM-induced disorder.

This work was supported in part by the Korean Department of Education under Grant No. BSRI 98-2440 and by the POSTECH research fund under Grant No. 1RB9910701.

[1] P. W. Anderson, Phys. Rev. **109**, 1429 (1958).
[2] N. F. Mott, *Metal-Insulator Transitions* (Taylor and Francis, New York, 1990), 2nd ed.
[3] J. Yi *et al.*, Phys. Rev. B **49**, 15 920 (1994).
[4] G. Y. Zimanyi *et al.*, Phys. Rev. Lett. **64**, 2719 (1990).
[5] M. Ma, Phys. Rev. B **26**, 5097 (1982).
[6] V. Dobrosavljević *et al.*, Phys. Rev. Lett. **78**, 3943 (1997).
[7] F. Flores *et al.*, Surf. Rev. Lett. **4**, 281 (1997).
[8] N. J. DiNardo *et al.*, Phys. Rev. Lett. **65**, 2177 (1990).
[9] J. M. Carpinelli *et al.*, Nature (London) **383**, 398 (1996).
[10] H. H. Weitering *et al.*, Phys. Rev. Lett. **78**, 1331 (1997).
[11] X. F. Lin *et al.*, Surf. Sci. **366**, 51 (1996).
[12] K. O. Magnusson *et al.*, Phys. Rev. B **41**, 12 071 (1990).
[13] H. H. Weitering *et al.*, Phys. Rev. B **48**, 8119 (1993); **45**, 9126 (1992).
[14] J. E. Northrup *et al.*, Phys. Rev. B **57**, R4230 (1998).
[15] U. del Pennino *et al.*, Phys. Rev. B **52**, 10 717 (1995).
[16] Oleg Pankratov *et al.*, Phys. Rev. Lett. **70**, 351 (1993).
[17] It is called an insulator (rather than a semiconductor) in a sense of nonvanishing energy gap.
[18] G. V. Hansson *et al.*, Surf. Sci. Rep. **9**, 197 (1988).
[19] Other line shapes including a Gaussian and a Lorentzian powered to 1 or 2 result in larger values for a "goodness of the fit" parameter.
[20] R. J. Birgeneau *et al.*, Phys. Rev. B **28**, 1438 (1983).
[21] J. W. Chung *et al.*, Phys. Rev. Lett. **59**, 2192 (1987).
[22] P. Laitenberger *et al.*, Phys. Rev. Lett. **76**, 1952 (1996).
[23] A. Clotet *et al.*, Phys. Rev. B **51**, 1581 (1995).
[24] H. Ibach and D. L. Mills, *Electron Energy Loss Spectroscopy and Surface Vibrations* (Academic Press, New York, 1982), p. 88.
[25] The state S_m appears slightly below E_F due to the finite temperature effect.